Efficient Design of Metamaterial Absorbers using Parametric Macromodels

Giulio Antonini[1], Maria Denise Astorino[2], Francesco Ferranti[3], Fabrizio Frezza[2], and Nicola Tedeschi[2]

[1]UAq EMC Laboratory, Dipartimento di Ingegneria Industriale e dell'Informazione e di Economia
Università degli Studi dell'Aquila, 67100 L'Aquila, Italy
giulio.antonini@univaq.it

[2]Department of Information Engineering, Electronics and Telecommunications
La Sapienza University of Rome, 00184 Rome, Italy
mariadenise.astorino@uniroma1.it, nicola.tedeschi@uniroma1.it, fabrizio.frezza@uniroma1.it

[3]Microwave Department
Institut Mines-Télécom Atlantique, CNRS UMR 6285 Lab-STICC, 29238 Brest CEDEX 3, France
francesco.ferranti@imt-atlantique.fr

Abstract – Metamaterial absorbers have recently attracted a lot of interest for applications spanning from microwave to terahertz, near infrared and optical frequencies, such as electromagnetic compatibility, thermal emitters, solar cells and micro-bolometers. In this paper, a procedure for the efficient design of metamaterial absorbers based on parametric macromodels is presented. These models are used to describe the frequency-domain behaviour of complex systems as a function of frequency and design parameters (e.g., layout features). Parametric macromodels are very efficient and can be used to speed up the design flow in comparison with using electromagnetic simulators for design tasks. The use of quasi-random sequences for the sampling of the design space and of radial basis functions and polynomial functions for the model construction is proposed. Numerical results validate the efficiency and accuracy of the proposed technique for multiple optimizations.

Index Terms – Efficient Design, Metamaterial Absorbers, Optimization, Parametric Macromodeling.

I. INTRODUCTION

Recently, metamaterial absorbers (MMAs) have aroused a huge interest and a large amount of research has been dedicated to the design of such devices [1] with specific characteristics ranging from the wide-angular response [2–4], to the polarisation insensitivity [4–8] and the bandwidth enhancement [9, 10]. Moreover, their applications span from microwave [11] to terahertz (THz) [12], near infrared and optical frequencies [13, 14], such as electromagnetic compatibility, thermal emitters [15], solar cells and micro-bolometers [16, 17].

The Salisbury screen was one of the first microwave absorbers [18], constituted of a resistive sheet and a dielectric layer backed by a metallic plate capable of achieving impedance matching with free space through quarter-wave antireflection interference, but with the disadvantage of a $\lambda/4$ thick dielectric spacer. Other examples, in the microwave range, are the Jaumann absorber [19] which exploits multiple resistive sheets to broaden the bandwidth and the high-impedance surfaces [20], i.e., periodic structures able to perform near-unity absorption at the desired frequency through the introduction of an amount of Ohmic or dielectric losses.

In the THz regime, instead, these absorbing devices are suitable for many applications in sensing, spectroscopy, monitoring, imaging and THz detectors, allowing to overcome the so-called "THz gap" [21, 22].

As pointed out in [23], it is not a challenging task to design an absorber working at a single frequency, at normal incidence, and with an arbitrary thickness. In the last decades, many efforts have been spent to reduce the absorbers thickness, and to improve the working bandwidth and the angular response. Moreover, another important property of an absorber is the polarisation insensitivity, i.e., the possibility to absorb the incident radiation independently of its polarisation. Several techniques have been implemented to achieve such requirements. Metamaterial absorbers, i.e., stratifi-

cations of metamaterial surfaces and dielectric slabs, usually allow to realize thin absorbers, at least for narrow-band applications. In order to obtain the polarisation insensitivity with a metamaterial absorber, it is enough to consider isotropic surfaces, i.e., isotropic unit cells in the directions transverse to the stratification one. In order to increase the bandwidth, the most common strategy is to superpose several layers, covering the upper layer with a dielectric superstrate [23–25].

Among the configurations of MMAs proposed in the literature, the most performable is composed of subwavelength frequency selective surfaces (FSSs) [24] printed on a grounded dielectric slab, i.e., a compact three-layer system in which the FSS is formed by electric ring resonators (ERRs) that allow controlling and independently tune the effective permittivity of the device.

While this setting has been found effective, to authors' knowledge its efficient optimization or design space exploration have never been addressed. These tasks are usually performed by multiple frequency-domain electromagnetic (EM) simulations for different design parameter values (e.g., layout features), trying to meet the desired requirements. It is also obvious that both design space exploration and optimization can be very time consuming since multiple EM simulations are needed, even for a single unit cell that is assumed to constitute a periodic structure.

In this paper, we focus on design optimization. In the literature, multiple optimization approaches have been proposed, e.g., based on particle swarm and genetic algorithms [26] and based on space mapping methods [27–31].

A different framework to efficiently and accurately perform design activities is based on parametric macromodels. These models [32–36] are able to accurately and efficiently model the behaviour of complex systems as a function of frequency (or time) and additional parameters (such as layout features). Once built, these models can be used to efficiently perform multiple design tasks such as design space exploration, optimization and variability analysis, which will otherwise result very computationally expensive if only based on EM simulations. We show that parametric macromodels are not only useful for a single design optimization, but they can be re-used to optimize the design to meet multiple sets of specifications. This is the main feature that distinguishes the proposed method from existing optimization methods proposed for EM systems. Also, the proposed technique leads to a model in a state-space form that provides an engineering interpretation: for example, poles and zeros of the system

transfer function can be computed and analyzed as a function of design parameters.

The paper is organised as follows. Section II briefly reviews the metamaterial absorbers with a special focus on the ultra-thin narrow-band MMA discussed in [37]. Then, the parametric macromodeling technique adopted to capture the dependence of the metamaterial absorber frequency-domain behaviour on the design parameters is presented in Section III. A design space composed of six design parameters has to be handled. We propose the use of quasi-random sequences for the sampling of the design space and of radial basis functions and polynomial functions for the model construction. Such a high-dimensional design space and model generation procedure have not been investigated in previous parametric macromodeling techniques. The effectiveness of the proposed approach is confirmed by the numerical results presented in Section IV. Finally, the conclusions are drawn in Section V.

II. METAMATERIAL ABSORBERS

The analysed ultra-thin narrow-band MMA with a four-fold rotational symmetry with respect to the incidence z-direction (see Fig. 1), follows a three-layer arrangement as discussed in [37, 38]. Its unit cell with a lattice constant $a = 80$ μm consists of a top metallic ERR and a lower ground plane separated by a 5.8 μm thick dielectric layer of benzocyclobutane (BCB) with relative permittivity ε_r = 2.5 and dielectric loss tangent $\tan\delta = 0.005$. Both the top and bottom layers are made up of lossy gold with a conductivity of 1×10^7 S/m and a thickness of 270 nm. In [37], an equivalent circuit is proposed in order to have a circuital (and more intuitive) interpretation of the EM phenomena related to the absorber. The numerical values of the circuit elements are identified only after the EM response of the absorber is obtained by an EM solver. Therefore, it is not a circuit model based on analytical equations, which can replace the EM solver to calculate the EM response of the absorber. It is to be noted that the equivalent circuit does not provide the same level of accuracy as the EM simulations.

In order to consider an infinitely periodic MMA, the unit cell has been simulated through the RF module of the EM solver of Comsol Multiphysics [39] based on the finite element method (FEM) applying Floquet periodic boundary conditions along the x and y axes and assuming an EM wave impinging at normal incidence along the z direction. We note that the use of a FEM solver is not mandatory for the proposed technique. Any EM solvers can be used. We employ perfectly matched layers (PMLs) on the top and bottom of the unit cell to absorb the excited

mode from the source port and any higher order modes generated by the periodic MMA along with port boundary conditions on the interior boundaries of the PMLs to retrieve the reflection and transmission coefficients in terms of scattering parameters. In fact, the absorbed power can be expressed as $A(\omega) = 1 - R(\omega) - T(\omega) = 1 - |S_{11}(\omega)|^2 - |S_{21}(\omega)|^2$, meaning that in a perfect MMA, the reflection and transmission need to be simultaneously minimised. Since, in this case, the backside is grounded by metallic plane thicker than the skin depth, the absorption equation reduced to $A(\omega) = 1 - R(\omega)$, and as the effective impedance is matched to the free space impedance, it is possible to obtain a perfect absorption at the resonant frequency on a wide angular spectrum. This behaviour can be reached by properly adjusting and selecting the geometric dimensions of the top ERR, the thickness and physical properties of the dielectric substrate, being these parameters responsible both for the electric and magnetic responses.
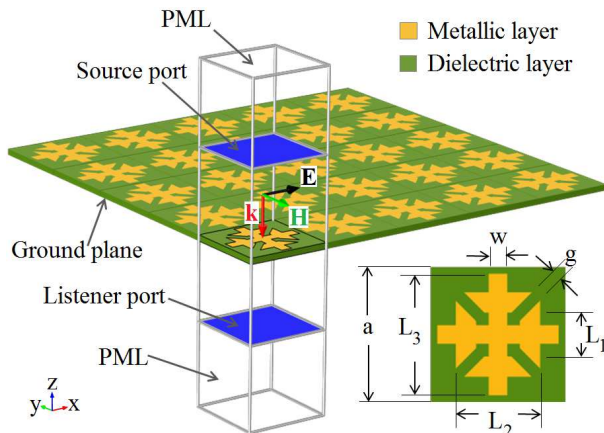

Fig. 1. Unit cell of the ultra-thin narrow-band MMA and virtual infinite 2D array.

In summary, the physical mechanism underlying this narrow-band MMA with a near unity absorption, is based on anti-parallel currents between the two metal layers that allow the coupling to the magnetic field, while the coupling to the incident electric field is due to the ERR that basically determines the absorption frequency. Indeed, when the electric field of the incident THz wave is parallel to one of the rods of the ERR, an electric dipole is excited on this rod, while no dipole exists on the orthogonal rod, but there is instead an electric-dipole resonance oscillating in anti-phase on the ground plane. Therefore, if the polarisation is not parallel to a particular rod, the electric dipoles of both rods will contribute to the absorption mechanism, giving results close to the case of parallel polarisation due to the symme-

try of the unit cell. In the following Section, we will determine the optimum set of geometric dimensions of the unit cell and the ERR able to guarantee the maximum absorption at a desired frequency.

III. PARAMETRIC MACROMODELING

In this Section, we describe the modeling method that will be used to generate parametric macromodels for efficient design. It aims to build a parametric macromodel $\mathbf{R}(s, \mathbf{g})$ that accurately describes the behaviour of a system as a function of the Laplace variable s and a set of design parameters $\mathbf{g} = (\mathrm{g}^{(m)})_{m=1}^M$, such as layout features. A parametric macromodel in the form:

$$\mathbf{R}(s, \mathbf{g}) = \mathbf{C}(\mathbf{g})\left(s\mathbf{I} - \mathbf{A}(\mathbf{g})\right)^{-1}\mathbf{B}(\mathbf{g}) + \mathbf{D}(\mathbf{g}), \quad (1)$$

is computed where $\mathbf{A}(\mathbf{g}) \in \mathbb{R}^{n_x \times n_x}$, $\mathbf{B}(\mathbf{g}) \in \mathbb{R}^{n_x \times n_u}$, $\mathbf{C}(\mathbf{g}) \in \mathbb{R}^{n_y \times n_x}$, $\mathbf{D}(\mathbf{g}) \in \mathbb{R}^{n_y \times n_u}$.

Let us consider a set of Q frequency-domain ($s = j\omega$) EM simulations at different values $\mathbf{g}_q$, $q = 1, ..., Q$ of the design parameters. In this paper, each EM simulation corresponding at the $\mathbf{g}_q$ sample provides the scattering parameters of the structure under study for a certain set of frequency samples $\mathbf{S}(j\omega_f, \mathbf{g}_q)$, $f = 1, ..., F$. Based on these frequency-domain data sets, a set of local linear time-invariant (LTI) state-space models $\mathbf{A}(\mathbf{g}_q), \mathbf{B}(\mathbf{g}_q), \mathbf{C}(\mathbf{g}_q), \mathbf{D}(\mathbf{g}_q)$ can be identified using any system identification techniques for LTI systems [40–42]. The local LTI models $\mathbf{R}(s, \mathbf{g}_q) = \mathbf{C}(\mathbf{g}_q)\left(s\mathbf{I} - \mathbf{A}(\mathbf{g}_q)\right)^{-1}\mathbf{B}(\mathbf{g}_q) + \mathbf{D}(\mathbf{g}_q)$ model the scattering parameters data $\mathbf{S}(j\omega_f, \mathbf{g}_q)$, $f = 1, ..., F$. The state-space matrices of the local LTI models can be interpolated as a function of $\mathbf{g}$:

$$\mathbf{A}(\mathbf{g}) = \sum_{q=1}^Q l_q(\mathbf{g})\mathbf{A}(\mathbf{g}_q), \mathbf{B}(\mathbf{g}) = \sum_{q=1}^Q l_q(\mathbf{g})\mathbf{B}(\mathbf{g}_q),$$

$$\mathbf{C}(\mathbf{g}) = \sum_{q=1}^Q l_q(\mathbf{g})\mathbf{C}(\mathbf{g}_q), \mathbf{D}(\mathbf{g}) = \sum_{q=1}^Q l_q(\mathbf{g})\mathbf{D}(\mathbf{g}_q)(2)$$

to obtain a parametric macromodel. The interpolation models can use interpolation functions $l_q(\mathbf{g})$ whose value is based on the distribution of the design parameters values $\mathbf{g}_q$ in the design space (e.g., multilinear interpolation [43]) and $\mathbf{A}(\mathbf{g}_q), \mathbf{B}(\mathbf{g}_q), \mathbf{C}(\mathbf{g}_q), \mathbf{D}(\mathbf{g}_q)$ are the state-space matrices estimated for the local LTI models identified at fixed design parameters values $\mathbf{g}_q$ [44]. Other interpolation models select a set of interpolation functions $l_q(\mathbf{g})$ and compute the matrix coefficients $\mathbf{A}_q, \mathbf{B}_q, \mathbf{C}_q, \mathbf{D}_q$ of the functions $l_q(\mathbf{g})$ by means of the solution of a linear system of equations (e.g.,

polynomial interpolation) [45, 46]:

$$\mathbf{A}(\mathbf{g}) = \sum_{q=1}^{Q} l_q(\mathbf{g})\mathbf{A}_q, \mathbf{B}(\mathbf{g}) = \sum_{q=1}^{Q} l_q(\mathbf{g})\mathbf{B}_q,$$

$$\mathbf{C}(\mathbf{g}) = \sum_{q=1}^{Q} l_q(\mathbf{g})\mathbf{C}_q, \mathbf{D}(\mathbf{g}) = \sum_{q=1}^{Q} l_q(\mathbf{g})\mathbf{D}_q. \quad (3)$$

We highlight that the matrix coefficients $\mathbf{A}_q, \mathbf{B}_q, \mathbf{C}_q, \mathbf{D}_q$ are different from $\mathbf{A}(\mathbf{g}_q), \mathbf{B}(\mathbf{g}_q), \mathbf{C}(\mathbf{g}_q), \mathbf{D}(\mathbf{g}_q)$.

In this work, we use an interpolation scheme based on radial basis functions and polynomial basis functions [47–49] where the interpolation for each entry of the state-space matrices can be written as:

$$\sum_{q=1}^{Q} w_q \phi(\mathbf{g} - \mathbf{g}_q) + \sum_{b=1}^{B} w_b p_b(\mathbf{g}). \quad (4)$$

Different radial basis functions $\phi(\mathbf{g}-\mathbf{g}_q)$ exist in the literature. In our work, we have chosen the multi-quadrics basis functions:

$$\phi(\mathbf{g} - \mathbf{g}_q) = \sqrt{r_q^2 + c^2}, \quad (5)$$

where r_q represents the euclidian distance between $\mathbf{g}$ and $\mathbf{g}_q$ and c is a positive parameter. The B polynomial functions have been chosen to be $[1, \mathrm{g}^{(1)}, \mathrm{g}^{(2)}, ..., \mathrm{g}^{(M)}]$ in our work.

The local LTI models are generated by independent system identification steps [40–42]. In this paper, we use the Vector Fitting (VF) technique [40] to first obtain pole-residue models for each design space samples $\mathbf{g}_q$:

$$\mathbf{S}(j\omega_f, \mathbf{g}_q) \simeq \mathbf{D}(\mathbf{g}_q) + \sum_{p=1}^{P} \frac{\mathbf{Res}_p(\mathbf{g}_q)}{j\omega - poles_p(\mathbf{g}_q)}. \quad (6)$$

Then, different state-space realization techniques can be used to generate the state-space matrices of the local LTI models $\mathbf{A}(\mathbf{g}_q), \mathbf{B}(\mathbf{g}_q), \mathbf{C}(\mathbf{g}_q), \mathbf{D}(\mathbf{g}_q)$ starting from the pole-residue models (6). The state-space representation of LTI models is unique up to a similarity transformation. The state-space matrices of the local LTI models need to be represented in a common state-space form to avoid potentially large variations as a function of the design parameters due to underlying similarity transformations, which might degrade the accuracy of the interpolation significantly. In the literature, several approaches have been proposed to transform the local LTI models into a state-space representation suitable for interpolation [35, 45, 46]. In this paper, we have used the barycentric realization discussed in [35].

If using one specific state-space realization would not provide the desired accuracy, then the technique [50] could be used to compute similarity transformation matrices that transform the set of local LTI models into a state-space form suitable to interpolation.

A. Design space sampling and model cross-validation

Multiple schemes can be used to choose the location of the Q samples in the $\mathbf{g}$ space. For example, Latin hypercube design [51] and quasi-random sequences [52]. Sobol and Halton sequences [52] are famous among quasi-random sequences. In this work, we have chosen the Sobol quasi-random sequence scheme [52]. Simple sampling schemes such as a regular tensor-product sampling will immediately provide a high number of samples as soon as the number of dimensions of the design space increases. Let us imagine to have M design parameters and to sample each design parameters interval with L samples. By taking the combination of all these samples (tensor-product), the total number of samples is equal to L^M. This is clearly not an efficient sampling scheme.

To estimate the accuracy of a parametric macromodel, of all Q simulations (then of all Q samples in the design space), a part of it is used to build the parametric macromodel (estimation) and another part is used to validate the model (validation). A scheme inspired by $k - fold$ cross validation is used to subdivide estimation and validation samples in the design space [53]. The set of Q simulations is randomly partitioned into k sets of approximately equal size. Then, for $i = 1, ..., k$, a parametric macromodel is built considering all but the $i - th$ data partition and the excluded dataset is used to evaluate the corresponding validation model error. An average validation model error based on the validation model errors of all the k iterations is used to estimate the average error over the design space for the parametric macromodel built by using all the data samples [53]. A $10 - fold$ ($k = 10$) cross validation has been used in this work. An illustration of the $10 - fold$ cross validation is provided in Fig. 2.
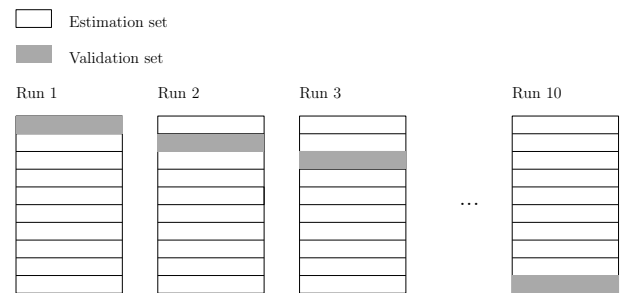

Fig. 2. 10-fold cross validation process.

Once the parametric macromodel is built, it can be used for design tasks, such as design optimization. The same model can be reused for different optimization tasks.

Concerning some computational considerations:

- if an EM solver-based approach is used, each iteration of a design optimization task leads to an EM simulation. Since each EM simulation can be computationally expensive, such an approach is very inefficient.

- Instead, in the case of the proposed technique, there is an initial computational cost needed to generate the parametric macromodel (the Q EM simulations previously mentioned). This initial computational effort becomes negligible when the model is used in multiple optimization cases. The parametric macromodel is an analytical model and therefore its evaluation is extremely fast. The same model is reused in multiple optimization tasks with different optimization objectives. This allows obtaining a very significant computational speed-up with respect to optimizations directly based on EM simulations. The proposed technique is based on system identification tools, interpolation schemes and cross-validation algorithms.

These computational considerations will be fully supported by numerical results in Section IV.

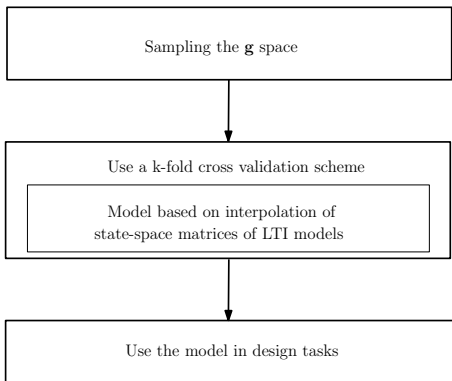Figure 3 summarises the main steps of the proposed modeling techniques.

Fig. 3. Main steps of the proposed modeling techniques.

IV. NUMERICAL RESULTS

A narrow-band MMA structure is used to validate the proposed modeling technique. The design parameters of the narrow-band MMA are: the lattice constant a, the gap g, the width w and the lengths L_1, L_2, L_3 which vary over the ranges [77-90] μm, [3-7] μm, [5-15] μm, [22-35] μm, [40-55] μm and [60-75] μm, respectively, as shown in Fig. 1. The 6D design space (a, g, w, L_1, L_2, L_3) includes 150 samples (Sobol sampling scheme) and each sample has required an EM simulation, examined over the frequency range [0.9-1.4] THz with a frequency resolution of 10 GHz (i.e., 51 frequency points for each simulation). In order to obtain the frequency-domain data samples of the reflection spectra for all 150 design space samples, it is necessary an overall CPU time equal to 237 h 30 m with an average CPU time for one EM simulation of about 1 h 35 m. Considering the 150 simulations, the VF technique [40] has been used to obtain pole-residue models (6) with $P = 6$ as number of poles. Figure 4 shows the location of the poles in the Laplace domain corresponding to the 150 pole-residue models.
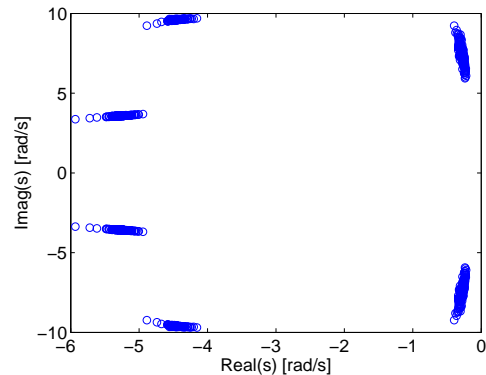
Fig. 4. Location of the poles in the Laplace domain corresponding to the 150 pole-residue models.

Then, the barycentric realization [35] has been used to generate the state-space matrices of the local LTI models $\mathbf{A}(\mathbf{g}_q), \mathbf{B}(\mathbf{g}_q), \mathbf{C}(\mathbf{g}_q), \mathbf{D}(\mathbf{g}_q)$ starting from the pole-residue models. Finally, an interpolation scheme based on multiquadrics radial basis functions and polynomial basis functions [47] has been used to construct the parametric macromodel.

A $10 - fold$ cross validation has been used to estimate the average absolute error of the final parametric macromodel in the design space. This estimated error is equal to 0.0208. The CPU time needed to perform the $10 - fold$ cross-validation and to build the final parametric macromodel using all data samples is equal to 58 s and 8.6 s, respectively. Then, the parametric macromodel has been used for three multiobjective optimizations whose objective is to achieve a maximum absorption at three different frequencies, namely $freq_{optim} = 1.1$ THz (Case I), $freq_{optim} = 1.2$ THz (Case II) and

Table 1: Optimal design parameters values (μm)

Case	a	g	w	L_1	L_2	L_3
I	78.68	4.61	12.67	27.59	52.89	73.13
II	82.66	5.67	12.60	27.09	49.66	69.87
III	84.99	5.06	12.75	26.78	45.57	66.76

Table 2: CPU time comparison

	Model Generation
EM FEM solver	
Proposed	150×1 h 35 m + 58 s + 8.6 s
	Optimization 1
EM FEM solver	9811×1 h 35 m
Proposed	84 s
	Optimization 2
EM FEM solver	10081×1 h 35 m
Proposed	88 s
	Optimization 3
EM FEM solver	$9451 \times$ 1 h 35 m
Proposed	82 s
	Speed-up
EM FEM solver	
Proposed	195x

$freq_{optim} = 1.3$ THz (Case III). Therefore, we have three optimization tasks. The function gamultiobj in Matlab$^{®}$ (R2014) has been used to run the three multiobjective optimizations with the default Matlab settings. The parametric macromodel has provided the value of S_{11} over a dense frequency grid of 501 points and for each design parameters value required by the optimizer. The obtained optimal values of the design parameters are shown in Table 1 for the three optimization cases.

To achieve these optimal values, the routine gamultiobj has required 9811, 10081 and 9451 function evaluations and a CPU time equal to 84 s, 88 s and 82 s using the parametric macromodel, respectively.

Three additional EM simulations have been performed to confirm the accuracy of the optimization results provided by the parametric macromodel. Figure 5 shows the absorbance response obtained by the parametric macromodel and the EM solver at the three optimal points. A very good agreement is achieved.
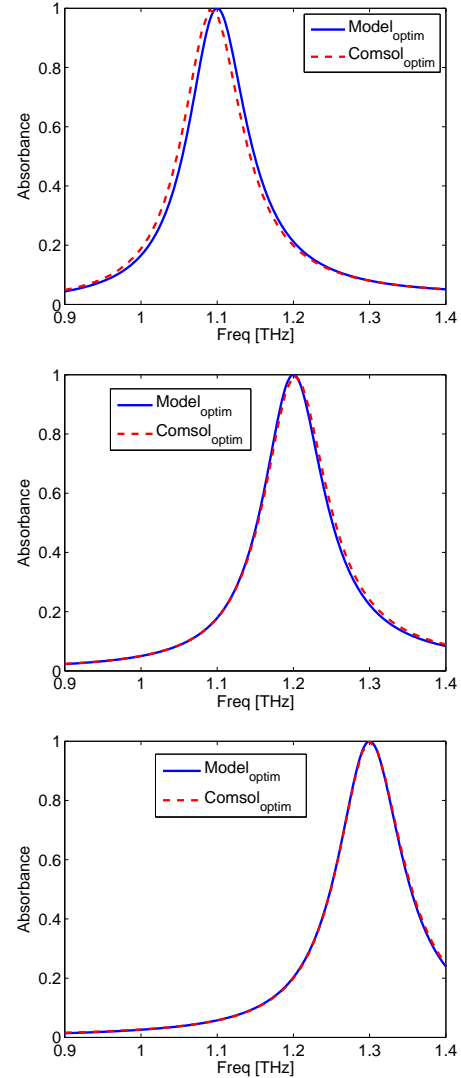
Table 2 summarizes the computational cost re-

Fig. 5. Optimization results: cases I-II-III (from top to bottom).

lated to 1) using Comsol and 2) using the proposed parametric macromodeling technique for the three optimization tasks. The speed-up obtained by using the proposed technique for the three optimizations is mentioned. It becomes evident that the initial computational effort for the parametric macromodel construction is justified by the very significant computational saving obtained for multiple design optimizations.

V. CONCLUSIONS

We have proposed an approach for the efficient design of metamaterial absorbers based on a parametric macromodeling technique. The interpolation of the state-space matrices of a set of LTI models is used to generate a parametric macromodel. This

is then used for different optimizations of an ultra-thin narrow-band metamaterial absorber. The numerical results confirm the efficiency and accuracy of the proposed technique, which allows computing optimal design values in a reduced amount of time.

REFERENCES

[1] Q. Wu, K. Zhang, and G. H. Yang, "Manipulation of electromagnetic waves based on new unique metamaterials: theory and applications," *ACES Journal*, vol. 12, pp. 977–989, December 2014.

[2] O. Luukkonen, F. Costa, C. R. Simovski, A. Monorchio, and S. A. Tretyakov, "A thin electromagnetic absorber for wide incidence angles and both polarizations," *IEEE Trans. Antennas Propag.*, vol. 57, no. 10, pp. 3119–3125, 2009.

[3] M. Diem, T. Koschny, and C. M. Soukoulis, "Wide-angle perfect absorber/thermal emitter in the terahertz regime," *Phys. Rev. B*, vol. 79, no. 3, p. 033101, 2009.

[4] S. Ghosh, S. Bhattacharyya, D. Chaurasiya, and K. V. Srivastava, "Polarisation-insensitive and wide-angle multi-layer metamaterial absorber with variable bandwidths," *Electronics Letters*, vol. 51, no. 14, pp. 1050–1052, 2015.

[5] H. Cheng, S. Chen, H. Yang, J. Li, X. An, C. Gu, and J. Tian, "A polarization insensitive and wide-angle dual-band nearly perfect absorber in the infrared regime," *J. Opt.*, vol. 14, no. 8, p. 085102, 2012.

[6] N. I. Landy, C. Bingham, T. Tyler, N. Jokerst, D. R. Smith, and W. J. Padilla, "Design, theory, and measurement of a polarization-insensitive absorber for terahertz imaging," *Phys. Rev. B*, vol. 79, no. 12, p. 125104, 2009.

[7] L. Lu, S. Qu, H. Ma, F. Yu, S. Xia, Z. Xu, and P. Bai, "A polarization-independent wide-angle dual directional absorption metamaterial absorber," *Prog. Electromagn. Res. M*, vol. 27, pp. 191–201, 2012.

[8] D. Chaurasiya, S. Ghosh, S. Bhattacharyya, A. Bhattacharya, and K. V. Srivastava, "Compact multi-band polarisation-insensitive metamaterial absorber," *IET Microwaves, Antennas & Propagation*, vol. 10, pp. 94–101, 2016.

[9] J. Sun, L. Liu, G. Dong, and J. Zhou, "An extremely broad band metamaterial absorber based on destructive interference," *Opt. Express*, vol. 19, no. 22, p. 21155, 2011.

[10] S. Gu, J. P. Barrett, T. H. Hand, B. I. Popa, and S. A. Cummer, "A broadband low-reflection metamaterial absorber," *J. Appl. Phys.*, vol. 108, no. 6, p. 064913, 2010.

[11] N. I. Landy, S. Sajuyigbe, J. J. Mock, D. R. Smith, and W. J. Padilla, "Perfect metamaterial absorber," *Phys. Rev. Lett.*, vol. 100, no. 20, p. 207402, 2008.

[12] J. Grant, S. S. Y. Ma, L. B. Lok, A. Khalid, and D. R. S. Cumming, "Polarization insensitive terahertz metamaterial absorber," *Opt. Lett.*, vol. 36, no. 8, pp. 1524–1526, 2011.

[13] G. Dayal and S. A. Ramakrishna, "Design of highly absorbing metamaterials for infrared frequencies," *Opt. Express*, vol. 20, no. 16, pp. 17503–17508, 2012.

[14] N. Liu, M. Mesch, T. Weiss, M. Hentschel, and H. Giessen, "Infrared perfect absorber and its application as plasmonic sensor," *Nano Lett.*, vol. 10, no. 7, p. 2342, 2010.

[15] X. Liu, T. Tyler, T. Starr, A. F. Starr, N. Jokerst, and W. J. Padilla, "Taming the blackbody with infrared metamaterials as selective thermal emitters," *Phys. Rev. Lett.*, vol. 107, no. 4, p. 045901, 2011.

[16] M. Laroche, R. Carminati, and J. J. Greffet, "Near-field thermophotovoltaic energy conversion," *J. Appl. Phys.*, vol. 100, no. 6, p. 063704, 2006.

[17] T. Maier and H. Bruckl, "Wavelength-tunable microbolometers with metamaterial absorbers," *Opt. Lett.*, vol. 34, no. 19, pp. 3012–3014, 2009.

[18] R. L. Fante and M. T. McCormack, "Reflection properties of the Salisbury screen," *IEEE Trans. Antennas Propag.*, vol. 36, no. 10, pp. 1443–1454, 1988.

[19] E. F. Knott and C. D. Lunden, "The two-sheet capacitive Jaumann absorber," *IEEE Trans. Antennas Propag.*, vol. 43, no. 11, pp. 1339–1343, 1995.

[20] S. A. Tretyakov and S. I. Maslovski, "Thin absorbing structure for all incident angles based on the use of a high-impedance surface," *Microwave Opt. Technol. Lett.*, vol. 38, no. 3, pp. 175–178, 2003.

[21] V. T. Pham, J. Park, D. L. Vu, H. Y. Zheng, J. Y. Rhee, K. Kim, and Y. P. Lee, "THz-metamaterial absorbers," *Adv. Nat. Sci. Nanosci. Nanotechnol.*, vol. 4, no. 1, p. 015001, 2013.

[22] C. Debus and P. Bolivar, "Frequency selective surfaces for high sensitivity terahertz sensing," *Appl. Phys. Lett.*, vol. 91, no. 18, p. 184102, 2007.

[23] C. S. Y. Ra'di and S. Tretyakov, "Thin perfect absorbers for electromagnetic waves: the-

ory, design, and realization," *Phys. Rev. Appl.*, vol. 3, p. 037001, 2015.

[24] B. A. Munk, *Frequency Selective Surfaces: Theory and Design*, Wiley, 2000.

[25] M. D. Astorino, F. Frezza, and N. Tedeschi, "Broad-band terahertz metamaterial absorber with stacked electric ring resonators," *J. Electrom. Waves Appl.*, vol. 31, no. 7, pp. 727–739, 2017.

[26] D.-H. Kwon, Z. Bayraktar, J. A. Bossard, D. H. Werner, and P. L. Werner, "Nature-inspired optimization of metamaterials," in *24th Annual Review of Progress in Applied Computational Electromagnetics*, April 2008.

[27] S. Koziel, "Multi-fidelity optimization of microwave structures using response surface approximation and space mapping," *ACES Journal*, vol. 24, pp. 600–608, December 2009.

[28] S. Koziel, J. Bandler, and Q. Cheng, "Robust trust-region space-mapping algorithms for microwave design optimization," *IEEE Transactions on Microwave Theory and Techniques*, vol. 58, no. 8, pp. 2166–2174, August 2010.

[29] S. Koziel and J. Bandler, "Fast design optimization of microwave structures using co-simulation-based tuning space mapping," *ACES Journal*, vol. 26, pp. 631–639, August 2011.

[30] S. Koziel, "Space mapping: Performance, reliability, open problems and perspectives," in *2017 IEEE MTT-S International Microwave Symposium (IMS)*, pp. 1512–1514, June 2017.

[31] S. Koziel and A. Bekasiewicz, "Reliable low-cost surrogate modeling and design optimisation of antennas using implicit space mapping with substrate segmentation," *IET Microwaves, Antennas and Propagation*, vol. 11, no. 14, pp. 2066–2070, 2017.

[32] F. Ferranti, L. Knockaert, and T. Dhaene, "Parameterized S-parameter based macromodeling with guaranteed passivity," *IEEE Microw. Wireless Compon. Lett.*, vol. 19, no. 10, pp. 608–610, October 2009.

[33] P. Triverio, S. Grivet-Talocia, and M. S. Nakhla, "A parameterized macromodeling strategy with uniform stability test," *IEEE Transactions on Advanced Packaging*, vol. 32, no. 1, pp. 205–215, February 2009.

[34] F. Ferranti, L. Knockaert, and T. Dhaene, "Passivity-preserving parametric macromodeling by means of scaled and shifted state-space systems," *IEEE Transactions on Microwave Theory and Techniques*, vol. 59, no. 10, pp. 2394–2403, October 2011.

[35] E. R. Samuel, L. Knockaert, F. Ferranti, and T. Dhaene, "Guaranteed passive parameterized macromodeling by using Sylvester state-space realizations," *IEEE Transactions on Microwave Theory and Techniques*, vol. 61, no. 4, pp. 1444–1454, April 2013.

[36] M. Kabir and R. Khazaka, "Parametric macromodeling of high-speed modules from frequency-domain data using Loewner matrix based method," in *IEEE MTT-S International Microwave Symposium*, pp. 1–4, June 2013.

[37] M. D. Astorino, F. Frezza, and N. Tedeschi, "Ultra-thin narrow-band, complementary narrow-band, and dual-band metamaterial absorbers for applications in the THz regime," *J. Appl. Phys.*, vol. 121, no. 6, p. 063103, 2017.

[38] M. D. Astorino, R. Fastampa, F. Frezza, L. Maiolo, M. Marrani, M. Missori, M. Muzi, N. Tedeschi, and A. Veroli, "Polarization-maintaining reflection-mode THz time-domain spectroscopy of a polyimide based ultra-thin narrow-band metamaterial absorber," *Scientific Reports*, vol. 8, no. 1, p. 1985, 2018.

[39] *COMSOL Multiphysics 4.4*, http://www.comsol.com/products.

[40] B. Gustavsen, "Improving the pole relocating properties of vector fitting," *IEEE Transactions on Power Delivery*, vol. 21, no. 3, pp. 1587–1592, 2006.

[41] L. Ljung, *System Identification: Theory for the User (2nd Edition)*, Prentice Hall, 1999.

[42] R. Pintelon and J. Schoukens, *System Identification: A Frequency Domain Approach*, Wiley-IEEE Press, 2012.

[43] W. A. Weiser and S. E. Zarantonello, "A note on piecewise linear and multilinear table interpolation in many dimensions," *Mathematics of Computation*, vol. 50, no. 181, pp. 253–264, January 1988.

[44] F. Ferranti, L. Knockaert, and T. Dhaene, "Guaranteed passive parameterized admittance-based macromodeling," *IEEE Trans. Advanced Packaging*, vol. 33, no. 3, pp. 623–629, August 2010.

[45] J. De Caigny, J. Camino, and J. Swevers, "Interpolation-based modeling of MIMO LPV systems," *IEEE Transactions on Control Systems Technology*, vol. 19, no. 1, pp. 46–63, 2011.

[46] J. De Caigny, R. Pintelon, J. Camino, and J. Swevers, "Interpolated modeling of LPV systems," *IEEE Transactions on Control Systems Technology*, vol. 22, no. 6, pp. 2232–2246, November 2014.

[47] M. D. Buhmann, *Radial Basis Functions*, Cambridge University Press, New York, NY, USA, 2003.

[48] G. Liu and Y. Gu, *An Introduction to Meshfree Methods and Their Programming*, Springer, 2005.

[49] G. R. Liu, *Meshfree Methods: Moving Beyond the Finite Element Method. Second Edition.*, CRC Press, 2010.

[50] F. Ferranti and Y. Rolain, "A local identification method for linear parameter-varying systems based on interpolation of state-space matrices and least-squares approximation," *Mechanical Systems and Signal Processing*, vol. 82, pp. 478–489, 2017.

[51] W.-L. Loh, "On Latin hypercube sampling," *Ann. Statist.*, vol. 24, no. 5, pp. 2058–2080, 1996.

[52] P. Brandimarte, *Low-Discrepancy Sequences*, pp. 379–401, John Wiley and Sons, Inc., 2014.

[53] T. Hastie, R. Tibshirani, and J. Friedman, *The Elements of Statistical Learning: Data Mining, Inference, and Prediction, Second Edition (Springer Series in Statistics)*, Springer, 2009.

Giulio Antonini received the Laurea degree (*cum laude*) in Electrical Engineering from the University of L'Aquila, L'Aquila, Italy, in 1994 and the Ph.D. degree in Electrical Engineering from University of Rome "La Sapienza" in 1998. Since 1998, he has been with the UAq EMC Laboratory, University of L'Aquila, where he is currently a Professor. His scientific interests are in the field of computational electromagnetics. He has coauthored the book "*Circuit Oriented Electromagnetic Modeling Using the PEEC Techniques*", (Wiley-IEEE Press, 2017).

Maria Denise Astorino received the B.S. and M.S. degrees in Electronic Engineering in 2012 and 2015, respectively, from the University of Rome "La Sapienza" where she is currently employed in the Ph.D. course in Mathematical Models for Engineering, Electromagnetics and Nanosciences. Her research interests include the study of microwave/THz periodic structures such as frequency selective surfaces and metamaterial absorbers through equivalent-circuit models, and the analysis of anisotropic media for applications in the electromagnetic cloaking effect.

Francesco Ferranti received the Ph.D. degree in Electrical Engineering from Ghent University, Ghent, Belgium, in 2011. He is currently an Associate Professor at the Microwave Department at Institut Mines-Télécom (IMT) Atlantique, Brest, France. His research interests include parameterized macromodeling and model order reduction, sampling techniques, design space exploration, uncertainty quantification, optimization, applied electromagnetics, behavioural modelling, microwave design and characterization, and multiphysics modeling.

Fabrizio Frezza received the Laurea degree (*cum laude*) in Electronic Engineering in 1986 and the Doctorate degree in Applied Electromagnetics and Electrophysical Sciences in 1991, both from "La Sapienza" University of Rome. In 1986, he joined the Department of Electronics of the same University, where he was Researcher from 1990 to 1998, temporary Professor of Electromagnetic Fields from 1994 to 1998, Associate Professor from 1998 to 2004, and he has been Full Professor of Electromagnetic Fields since 2005. His research activity has concerned guiding structures, antennas and resonators for microwaves and millimeter waves, numerical methods, scattering, optical propagation, plasma heating, anisotropic media, artificial materials and metamaterials, cultural-heritage applications. Dr. Frezza is a Member of Sigma Xi and Senior Member of IEEE and OSA.

Nicola Tedeschi received the Master degree in Electronic Engineering, from "La Sapienza" University of Rome in 2009. He received the Ph.D. in Electromagnetics from the same University in 2013. He was visiting student in the Department of Radio Science and Engineering of the Aalto University, Espoo, Finland, in 2012. His research interests concern microwave amplifiers, electromagnetic scattering by objects near to interfaces, propagation of inhomogeneous waves in dissipative media, and the characterization of dispersive properties of natural and artificial materials.